RSC Advances

PAPER

View Article Online
View Journal | View Issue

Cite this: *RSC Adv.*, 2021, **11**, 32494

Enhanced sorption of the UV filter 4-methylbenzylidene camphor on aged PET microplastics from both experimental and theoretical perspectives†

Chun-Yu Shih, [a] Yu-Hsiang Wang, [a] Yi-Ju Chen,[a] Hsin-An Chen [b] and Angela Yu-Chen Lin*[a]

In this study, the morphology and sorption behavior of polyethylene terephthalate (PET) microplastics during the aging process are investigated. To clarify the sorption mechanism of aged PET microplastics, the common sunblock 4-methylbenzylidene camphor (4-MBC) was chosen as the target contaminant, and UV irradiation was used for the laboratory aging simulation. The results show that oxygen-containing functional groups (carboxylic, carbonyl, ketone and hydroxyl groups) increase on the surface of aged PET microplastics. Based on density functional theory (DFT) simulations, the camphor part of 4-MBC acts as a hydrogen bond acceptor, whereas the carboxylic group on aged PET microplastics acts as a hydrogen bond donor. The formation of hydrogen bonding causes increased sorption of 4-MBC on aged PET microplastics. The sorption capacity increased from 5 to 11 μg g^{-1} for 50 ppb 4-MBC with 100 mg PET microplastics after a five-day aging process. Other environmental factors that affect sorption were also identified; a higher pH value and the presence of salinity reduced the amount of sorption. The sorption of virgin PET ranged from 8.0 to 3.4 μg g^{-1} and the sorption of aged PET ranged from 22 to 5 μg g^{-1} at pH 4 to 10. In the presence of salinity (10% seawater), the virgin PET sorption dropped to 2.1 μg g^{-1} while the aged PET sorption dropped to 4 μg g^{-1}. A similar phenomenon was also observed in the sorption behavior under natural sunlight (the sorption of PET increased from 0.4 to 0.8 μg g^{-1} after 6 months of aging). The potential risk to ecosystems of aged PET microplastics under prolonged sunlight exposure in the natural environment could be greater than that predicted for virgin microplastics.

Received 29th June 2021
Accepted 27th September 2021

DOI: 10.1039/d1ra05013c

rsc.li/rsc-advances

1. Introduction

Microplastics are plastic fragments with a size less than 5 mm.[1] They have been widely found in aquatic environments, such as oceans, lakes, rivers, and wastewater treatment plants. Microplastics may pose threats to human health through the food chain due to plastic ingestion by marine species and seabirds and may further affect the circulatory system and endocrine system of marine organisms.[2,3] Moreover, various contaminants have also been reported to adsorb onto microplastics. With the uptake of contaminants onto microplastics, several studies[4–6] have indicated that microplastics act as a vector to accumulate contaminants, thereby transporting them over a wide range[7] and leading to the high bioavailability of pollutants to organisms when consumed. Hence, microplastic-sorbed contaminants in aquatic systems might represent one of the most threatening issues nowadays.

The morphology and chemical structure of microplastics can be easily affected by solar irradiation, heat, chemical oxidation and biodegradation.[8,9] Therefore, observed microplastics are aged under most conditions, and studies performed using virgin microplastics may underestimate the risk of contaminants adsorbed onto aged microplastics. Previous studies have revealed that the difference between aged microplastics and virgin microplastics is caused by alterations in physicochemical properties, including both structural[10–13] (*e.g.*, surface area, crystallinity and surface roughness) and surface chemical properties[14–17] (*e.g.*, functional groups and electrostatic interactions). Liu *et al.*[16] found that the mobility of aged microplastics in the environment is greater than that of virgin microplastics because of the increased surface oxidation of aged microplastics, which enhances the surface charge and hydrophilicity. In these circumstances, the transmission range

[a]*Graduate Institute of Environmental Engineering, National Taiwan University, 71-Chou-Shan Road, Taipei 106, Taiwan, Republic of China. E-mail: yuchenlin@ntu.edu.tw; Tel: +886-2-3366-4386*

[b]*Institute of Materials Science and Engineering, National Taipei University of Technology, 1, Sec. 3, Zhong-Xiao E. Rd., Taipei 106, Taiwan, Republic of China*

† Electronic supplementary information (ESI) available. See DOI: 10.1039/d1ra05013c

of contaminants will increase. Consequently, as more marine organisms ingest microplastics and absorb contaminants, more harm will be caused to these organisms.[18–20]

4-Methylbenzylidene camphor (4-MBC) is a commonly used organic UV filter added to plastic personal care products to reduce the harm of radiation to human skin.[21] Studies[22–25] also indicate that 4-MBC can be easily uptaken by microplastics because of its hydrophobicity, and microplastics thereby become a platform transporting this contaminant into aquatic environments. Several studies[26–28] have shown that 4-MBC can exert adverse effects on the reproduction and development of marine species at environmentally relevant concentrations. Additionally, 4-MBC is believed to disperse adsorbed UV energy and persist under UV radiation due to the isomerization between the (*E*)- and (*Z*)-isomers, which has recently raised significant concerns about its environmental stability.[23,29–31] In addition, Beiras *et al.*[32] indicated that microplastics could be vectors ingested by marine species. Therefore, 4-MBC was selected as a model contaminant to investigate the sorption behavior of aged microplastics.

Researchers have different opinions regarding the effect of aging on the sorption capacities;[8,33–36] the detailed mechanisms that alter the sorption behavior of aged microplastics remain a topic of discussion. Some studies have reported that the sorption capacity of microplastics decrease after aging, with an increase in the hydrophilicity of the surface of the polymer between microplastics and hydrophobic organics.[37,38] Hydrogen bonding between microplastics and water can also decrease the sorption capacities of contaminants.[8] On the other hand, others have demonstrated that the sorption capacity of aged microplastics is larger than that of virgin microplastics because of an increase in the surface area after aging.[12,39–41] An increase in crystallinity can cause the softer aged microplastics to absorb contaminants more easily.[41] The electrostatic attraction of aged microplastics with contaminants after the effect of the aging process on the zeta potential of microplastics was indicated as another factor enhancing the sorption behavior.[35,40,42] Studies reported that an increase in the hydrophilicity of the polymer between microplastics and contaminants can increase the uptake of contaminants by microplastics.[17,34,41,43] Previous studies have also proposed that the increase formation of oxygen-containing functional groups on the surface of microplastics can enhance the sorption behavior of aged microplastics by hydrogen bond generation;[12,34,35,39,43] however, currently, no study has identified the specific oxygen-containing functional groups that affect the sorption behavior. Density functional theory (DFT) has been used to study electrostatic repulsion at the molecular level for microplastic sorption.[44–46] DFT is also a very effective tool for simulating hydrogen bonds.[47–49] However, this type of simulation of hydrogen bonds has not yet been used for microplastics.

Consequently, the specific objectives of this study were to (1) investigate the sorption behavior of 4-MBC onto virgin and aged microplastics; (2) identify the specific oxygen-containing functional groups generating hydrogen bonds between 4-MBC and microplastics by DFT; (3) classify hydrogen bond formation from an experimental viewpoint; and (4) investigate the effect of environmental factors on 4-MBC sorption. In this pilot study, both experimental and theoretical viewpoints were discussed in depth; DFT was used as a theoretical way to identify the specific oxygen-containing functional groups that generate hydrogen bonds affecting the sorption behavior of aged microplastics, and acetonitrile solution was used experimentally to estimate the formation of hydrogen bonds during sorption.

2. Materials and methods

2.1 Materials and chemicals

Plastic particles of high-density polyethylene (HDPE) were purchased from the USI Corporation, polypropylene (PP) was purchased from the LCY Chemical Group, and polyethylene terephthalate (PET) was purchased from the Shinkong Synthetic Fibers Corporation. Bottled PET (Bot-PET) samples were purchased from UNI Water of Uni-President Enterprises Corporation in Taiwan. HDPE, PP and PET samples were further milled in a cryomill (Retsch, Germany) into crushed form and homogenized to achieve particle sizes of 150 to 200 μm. All three types of microplastics were washed with methanol to remove any existing contaminant chemicals and dried with liquid nitrogen before use.

Gradient-grade acetonitrile (ACN) and methanol were purchased from Merck (Darmstadt, Germany) with a minimum purity of 99%. 4-MBC with a minimum purity of 99% was obtained from Sigma-Aldrich (USA), and its physicochemical properties are listed in Fig. S1.† A stock solution of 4-MBC was prepared in 100% methanol and stored in the dark at −20 °C, and the stock solution was refreshed every four months. Artificial sea salt (S9883) was purchased from Sigma-Aldrich (Taufkirchen, Germany) with mass fractions of 55% Cl^-, 31% Na^+, 8% SO_4^{2-}, 4% Mg^{2+}, 1% K^+, 1% Ca^{2+} and <1% other. Ultrapure water (resistance of 18.2 MΩ cm; Millipore Co., MA, USA) was used to prepare all solutions.

2.2 Sorption batch experiments

All batch experiments were performed in 110 mL amber glass bottles with polytetrafluoroethylene (PTFE) caps as the reactor systems and prepared in ultrapure water to avoid biodegradation and photooxidation. For each sample, 100 mg of microplastics was prewetted with 30 mL of 0.01 M $CaCl_2$, which served as a bacteriostatic agent, for 12 h. Each reactor was spiked with 30 mL of a methanol solution containing 4-MBC. The relative volume of methanol in the aqueous solution was kept beneath 0.2% (v/v) to reduce cosolvent effects for all the samples.[50] The initial concentration of contaminants was set at 50–1500 μg L^{-1}. Bottles were capped and stirred well (1000 rpm) with a magnetic stirrer in the dark at 20 °C for 27 h, as experiments showed that sorption equilibrium was reached within 24 h. Samples were taken periodically, and an equal amount of ACN was added to form a 50 : 50 (v/v) ACN solution to avoid depositing the remaining 4-MBC on the Agilent PTFE filter. The samples were then filtered through 0.2 μm Agilent PTFE filters to separate the aqueous solution and microplastics within 30 seconds to prevent the desorption of 4-MBC into the aqueous solution. The

scheme of the sorption experiment is shown in Fig. S2.† All experiments were performed in duplicate.

To study the effect of pH, the initial pH values of the background solution mixed with $CaCl_2$ and 4-MBC were adjusted to pH 4, 6, 8 and 10 by using NaOH (0.1 M) or HCl (0.1 M). Simulated seawater was produced by dissolving artificial sea salt in water to study the effects of salinity, and the concentration of simulated seawater was set at 3.5‰ (w/w). To study the effects of water on hydrogen bond formation, an aqueous reaction solution was prepared with ACN instead of water. In the three experiments above, the initial concentration of contaminants was set at 50 μg L^{-1}, and the microplastic content was 100 mg in 60 mL amber glass bottles.

2.3 Aging process and characterization of microplastics

Microplastics were exposed to UV light (4 × 16 W UV lamps with a maximum wavelength of 254 nm) for 120 h for the laboratory aging (lab-aging) process (Fig. S3†). For the *in situ* aging process, Bot-PET samples were placed on the roof of the Graduate Institute of Environmental Engineering (GIEE) building (GPS coordinates: 25.0180, 121.5433; Taiwan) for predetermined time intervals (0, 3, 6, 9, and 12 months); the Env-PET sample was a PET bottle collected on a beach in Yilan, Taiwan (GPS coordinates: 24.8567, 121.8327; Taiwan), in February 2019. More climate information is provided for the sampling sites in Text S1.† The aged samples were washed with ultrapure water, filtered through 0.8 μm cellulose acetate filter paper, freeze-dried for 3 h and collected for use in sorption batch experiments. The physical dimensions and morphologies of the microplastics were characterized by field emission scanning electron microscopy (FESEM, SU-8010, Hitachi, Japan) operated at an acceleration voltage of 10 kV. The scanning electron microscope (SEM) samples were prepared by dispersing a small amount of microplastics in ethanol, adding a drop to a silica-coated glass sample holder and coating with a layer of gold. The sample-containing glass microscope slides were oven dried at 90 °C before performing the SEM measurements. The coated samples were analyzed by using a 10 kV acceleration voltage, and images were obtained at 40 000 times magnification. Fourier transform infrared (FTIR) spectroscopy and X-ray photoelectron spectroscopy (XPS) were employed to provide surface elemental identification. Spectroscopic analyses were performed using a Nicolet iS50 (Thermo Scientific, UK) to collect FTIR data. Each sample was analyzed in the attenuated total reflectance (ATR) mode. IR spectra were measured using a mercury cadmium telluride (MCT) single element detector at a spectral resolution of 16 cm^{-1} with a wavenumber range of 4000–500 cm^{-1}. XPS analysis was performed with a JPS-9030 (JEOL, Ltd, Japan) equipped with a monochromatic Al Kα radiation source (1486.7 eV). Charge compensation was achieved with a flood source. The survey and high-resolution spectra were recorded at a take-off angle of 45° in fixed analyzer transmission mode with pass energies of 100 and 20 eV, respectively. The C 1s and O 1s electron binding energies were determined for the different carbon and oxygen species. The concentrations of target compounds in experimental samples were analyzed by liquid chromatography-tandem mass spectrometry (LC-MS/MS) with an Agilent 1200 liquid chromatograph (Agilent, Palo Alto, CA, USA) equipped with a ZORBAX Eclipse XDB-C_{18} column (150 × 4.6 mm, 5 μm pore size). Further details of the LC-MS/MS instrument conditions and data analysis of the sorption experiment are described in ESI Text S2 and S3.†

2.4 Density functional theory studies

In this study, series of simulations with the goal of clarifying the interactions between 4-MBC water (H_2O), carboxylic (RCOOH), alcohol (RCOH) and aldehyde (RCHO) groups moieties were performed by using the Vienna *ab initio* simulation package (VASP) based on DFT.[51–53] The generalized gradient approximation (GGA) was used with the Perdew–Burke–Ernzerhof (PBE)[54,55] exchange-correlation functional and the projector augmented wave (PAW)[56,57] pseudopotentials.

The kinetic energy cut-off for the plane-wave basis set of wave functions was set to 400 eV. The self-consistent field convergence criterion for energy was set to be $dE < 10^{-5}$ eV, where atomic forces were minimized to $F_{max} < 10^{-2}$ eV $Å^{-1}$. To describe weak interactions, such as hydrogen bonding and van der Waals (vdW) interactions, in the modeling system, DFT-D3 with Becke–Jonson damping[58,59] was introduced as a semi-empirical dispersion correction for the energy. The binding energy (E_b) between 4-MBC and the selected molecules was defined by $E_b = E_{sys} - (E_1 + E_2)$, where E_{sys} stands for the total energy of the whole system and E_1 and E_2 stands for the total energy of the individual part, respectively.

3. Results and discussion

3.1 Physical and chemical characterization of aged PET microplastics

Fig. 1 shows SEM images of PET microplastics after aging in 4 × 16 W UVC light for 120 h. The results indicate that wrinkles occurred on the aged PET microplastics after the aging process, which could increase sorption by increasing the surface area.

In addition to causing the development of wrinkles, the aging process may also have affected the chemical properties of the microplastics. The XPS results for the virgin and aged PET microplastics show that both the content of oxygen-containing functional groups and the oxygen/carbon (O/C) ratio on the PET microplastics increased after the aging process (Table S5† and Fig. 2). The O/C ratio is a parameter to quantitatively describe the surface alteration properties of microplastics and is significantly correlated with the polymer types.[17] The XPS data showed that the intensity of O/C increased (63.7% > 57.6%) after the aging process. In particular, the C–O (16.7% > 15.2%) and carbonyl bands (22.2% > 21.4%) increased, while the C–H bonds decreased (63.5% > 61.1%) after the simulated aging process, which reveals that the PET was oxidized. This is basically consistent with the results of previous studies[14,43,60] on the artificial aging process of microplastics. Additionally, these phenomena are consistent with data obtained in previous studies[61–63] in which photodegradation cleaved chemical bonds

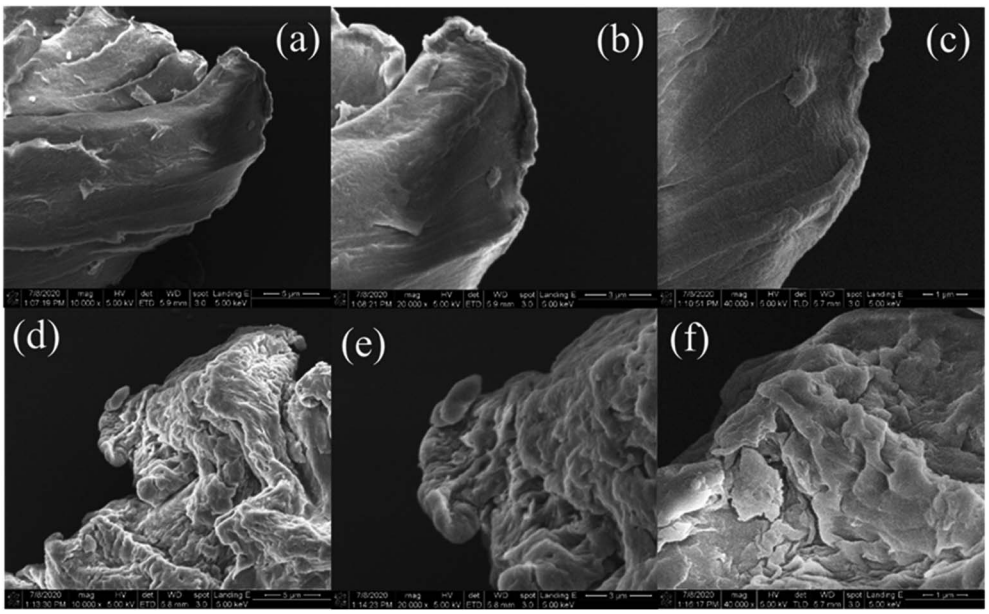

Fig. 1 SEM images of virgin (upper) and aged (lower) PET microplastics. Enlarged: 100 00× (a and d), 200 00× (b and e) and 400 00× (c and f).

in the main polymer chain and produced free radicals (peroxy radicals and polymer radicals) that reacted with oxygen and formed an inert product that reacted with the polymer, therefore reducing C–H and C=C bonds. Meanwhile, the XPS data verified the aging process of PET particles.

After increases in the O/C ratio were observed from the XPS data, further investigations of the related oxygen-containing

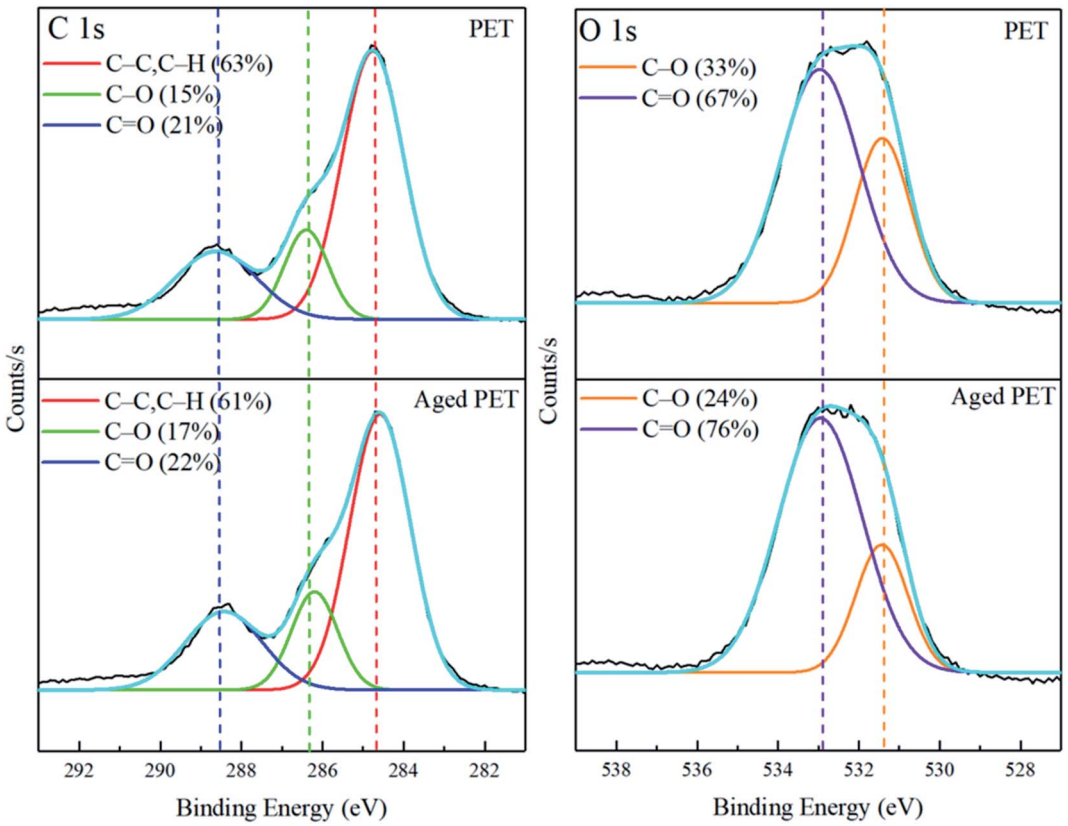

Fig. 2 XPS spectra of the C 1s orbital and O 1s orbital of virgin and aged PET microplastics.

functional groups were conducted with FTIR. Fig. 3 shows the FTIR spectra of virgin and aged PET microplastics, and the characteristic peak at 1100 cm^{-1} is attributed to C–O stretching. The stretching vibration of the –OH group produces a peak at 3400 cm^{-1}, and C–H bending produces a peak at 700 cm^{-1}. The peaks at 1450 cm^{-1} and 1730 cm^{-1} could be as associated with C–O and C=O stretching, respectively.[64,65]

Since the carbonyl index, calculated by the ratio of the absorption intensity of carbonyl group (1730 cm^{-1}) to that of methylene (1450 cm^{-1}), can represent the degree of aging of microplastics and can strongly affect the sorption behavior of aged microplastics based on observations made in earlier studies,[8,17,41] it can be inferred that functional groups with carbonyl groups, such as carboxylic groups (RCOOH), carbonyl groups (RCHO), ketone groups (RCOR) and hydroxyl groups (RCOH), may have affected the sorption of 4-MBC. As shown in Table S5,† the carbonyl index value of aged PET was higher than that of virgin PET, which further confirmed the oxidation of PET during the aging process. There was a significant increase in the abundance of the RCOOH peak in PET due to the aging process; notably, RCOOH is the final oxidation byproduct of primary alcohol oxidation (the intermediate oxidation byproducts are ketone groups (RCOR) and aldehyde groups (RCHO)). Therefore, the significant increase in RCOOH abundance in PET agreed with the O/C ratio and SEM results. The results also show that C–H and C=C bonds within the polymer chains break during the aging process, and the corresponding FTIR peaks at wavenumbers of 1350 and 1730 cm^{-1}, respectively, were lower for the aged PET microplastics than for the virgin PET microplastics and consistent with the XPS data.

According to previous studies, the surface oxygen-containing functional groups in aged PET microplastics may form hydrogen bonds with 4-MBC, strengthening the sorption of 4-MBC.[33,66–69] However, the O/C ratio has a positive correlation with the sorption of hydrophilic antibiotics,[17,70] and the hydrophobic sites on microplastics could be reduced by surface oxidation. Hence, the sorption of contaminants by microplastics can be affected by hydrophobic interactions between these compounds. Nevertheless, several studies[22,34,40,71] have mentioned that the sorption behavior between microplastics and hydrophilic organic contaminants is more strongly dominated by hydrogen bonding than by hydrophobic interactions. Thus, this study concentrates on exploring the effect of hydrogen bonding between virgin and aged PET microplastics and 4-MBC in the following section.

3.2 Effect of PET microplastic aging on sorption and sorption isotherms

3.2.1 Effect of PET microplastic aging on sorption. To investigate the hypothesis regarding the greater sorption of 4-MBC by aged PET microplastics than virgin PET microplastics, sorption tests were performed by mixing 100 mg of PET microplastics with 50 ppb 4-MBC. In the sorption experiment (Fig. 4), the sorption of 4-MBC by aged PET microplastics (11 μg g^{-1}) was higher than that by virgin PET microplastics (5 μg g^{-1}). Additionally, based on analysis of the entire sorption process, sorption equilibrium was reached in 24 h. The increase in the sorption confirmed that the presence of oxygen-containing surface functional groups on aged PET microplastics allowed for the formation of hydrogen bonds with 4-MBC.

The kinetic parameters, including the sorption capacity at equilibrium (q_e), rate constant (k), and regression coefficient (R^2) derived from the pseudo-second order and pseudo-first order models, are listed in Table S6.† It is worth noting that the sorption kinetics fit the pseudo-second order model with regression coefficient (R^2) values > 0.99. The rate constant of the fitted pseudo-second order model was 20% greater for aged PET than for virgin PET. The acceleration in sorption may have been affected by the formation of oxygen-containing functional groups and crack formation, as these processes increased the active sorption sites on the aged PET microplastics. Similar

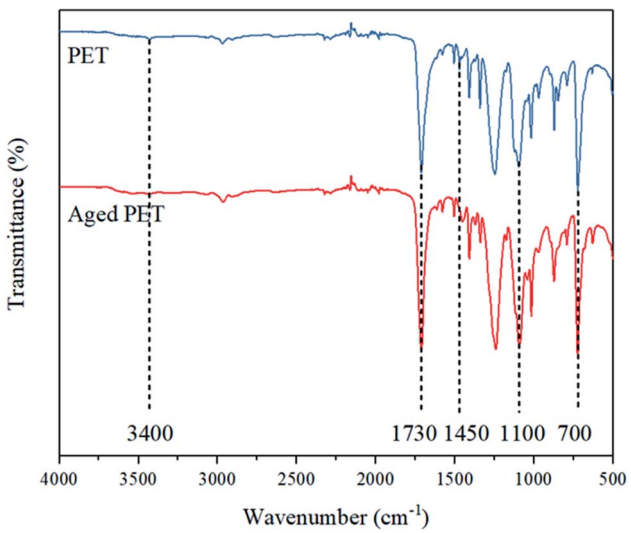

Fig. 3 FTIR spectra of virgin and aged PET microplastics.

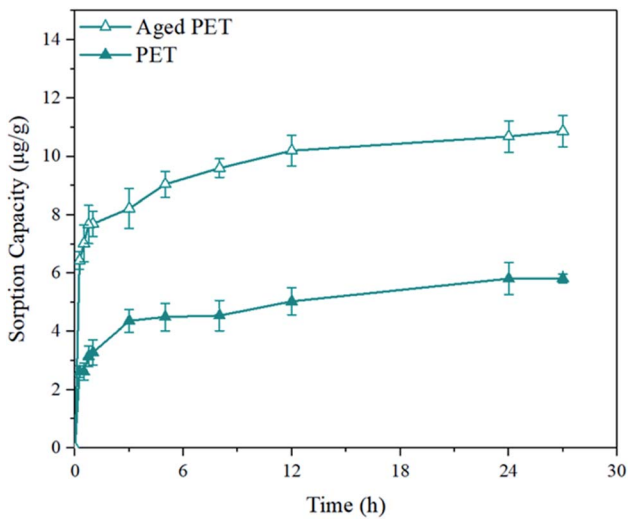

Fig. 4 Sorption kinetics of virgin and aged PET microplastics with 4-MBC over 27 h ($[4\text{-MBC}]_0$ = 50 ppb, $[\text{microplastics}]_0$ = 100 mg, temperature = 20 °C, initial pH = 7, salinity = 0).

development was also observed in previous studies,[72,73] in which sorbents with carboxylic groups had faster sorption rates than those without carboxylic groups due to the affinity between the sorbent and sorbate.

To further investigate the sorption kinetics of 4-MBC onto PET microplastics, the data for the fitted pseudo-second order model at 20 °C and 50 °C were then used to calculate the sorption activation energy. The Arrhenius equation was used to calculate the sorption activation energy, and the results are shown in Table S7.† The activation energy of aged PET microplastics at temperatures between 20 °C and 50 °C was half of virgin microplastics. Additionally, the sorption of virgin and aged PET both decreased with increasing sorption temperature. The lower activation energy of aged PET microplastics showed that aged PET microplastics will adsorb 4-MBC faster than virgin PET microplastics, which is also consistent with the results in Table S6.† With the same sorption mechanism, Koyuncu *et al.*[74] also discovered that the sorption decreases as the sorption temperature increases, in which the sorption of acid activated kaolinites with 3-methoxybenzaldehyde with hydrogen bonding formation.

3.2.2 Sorption isotherms. Several studies have investigated the sorption behavior between organic contaminants and microplastics, including both linear isotherms[33,75] and Langmuir isotherms.[76,77] Langmuir sorption parameters, Freundlich sorption parameters and regression coefficient (R^2) values for PET microplastics were estimated and are reported in Fig. S4 and S5.† The PET sorption data were fitted better by the Langmuir isotherm than the Freundlich isotherm (R^2: 0.999 > 0.997).

The good fit to the Langmuir model shows that the PET microplastics all exhibited monolayer sorption and that all sites had the same reaction energy, which means that the sorption processes were dominated by chemical sorption.[67,68,78,79] Furthermore, high correlations between monolayer sorption and the hydrogen bonding acting force have been observed in previous works.[80,81] The good fitting results in the present study suggest that the oxygen-containing functional groups generated on the surface of PET microplastics easily formed hydrogen bonds with 4-MBC, especially in aged PET microplastics.

3.3 Mechanism of the sorption process due to hydrogen bonds

3.3.1 DFT simulations of 4-MBC and PET microplastics. By comparing the FTIR spectra of the virgin and aged PET microplastics, we found that oxygen-containing functional groups (RCOOH, RCHO and RCOH) increased during the aging process, which may have increased the 4-MBC sorption of the aged PET microplastics by forming hydrogen bonds. Several methods can be used to characterize hydrogen bonds, as mentioned by Ahmed and Jhung.[82] However, due to the low sorption capacity of most of the environmental samples, it was difficult to evaluate the presence of hydrogen bonds by experimental methods. Therefore, DFT calculations were employed to determine the binding energies between the considered functional groups (RCOOH, RCHO, water and RCOH) and 4-MBC, providing deep insight into 4-MBC sorption on the surface of PET microplastics from an atomic viewpoint.

Since 4-MBC can only be a hydrogen acceptor in hydrogen bond formation, the target oxygen-containing functional group should act as a hydrogen donor in the reaction. Table S8† lists the calculated binding energies between the functional groups and 4-MBC. Note that the keto–enol transformation of 4-MBC was ignored because the rigid body of the benzene ring suppressed such transformation.

RCOOH has the largest binding energy, twice those of RCHO and RCOH, indicating that RCOOH is the main functional group that affects the formation of hydrogen bonds. In addition, the resonance of the carboxylic group creates two latent positions on the RCOOH moiety that can form hydrogen bonds with 4-MBC. This observation suggests that RCOOH would be the most effective functional group for hydrogen bond formation. These results also agree well with the enhanced sorption of aged PET microplastics for 4-MBC.

3.3.2 Sorption in ACN solution. We replaced water with ACN as the solvent to evaluate the effect of the solvent in the solution on hydrogen bond affinities with 4-MBC, as shown in Fig. 5a. The results indicate that the sorption of 4-MBC in ACN is lower than that in water (the sorption of virgin PET decreased from 5.3 to 1.2 μg g^{-1}, and the sorption of aged PET decreased from 10.9 to 3 μg g^{-1}). The sorption of 4-MBC onto PET microplastics in the ACN solution was relatively low, only one-third that in water. Casillas-Ituarte and Allen[83] also revealed that atrazine served as the hydrogen acceptor in hydrogen bonding with the silanol group on the surface of silica and had a lower sorption capacity for atrazine in the ACN solution because of the lower hydrogen bond affinity in the ACN solution than in water.

Since the water that served as the hydrogen donor had been removed from the reaction, the sorption ratio between aged PET microplastics and virgin PET microplastics increased in the ACN solution (the sorption capacity of aged PET was twice that of virgin PET in water but threefold in the ACN solution). This variation could be attributed to the formation of RCOOH, which generates hydrogen bonds, during the aging process. Moreover, the potential impact of aged PET in the environment was revealed by its 4-MBC sorption behavior, which is dominated by hydrogen bonding with RCOOH.

3.4 Effect of environmental factors

3.4.1 Effect of pH. Although 4-MBC sorption is dominated by hydrogen bonds formed with RCOOH on the surface of aged PET microplastics, it may also be affected by environmental factors such as pH, salinity, and weather. The pH value has an impact on the charge on the surface and sorbates and thus affects the sorption behavior by the electrostatic force. The effect of pH on the sorption of 4-MBC onto PET microplastics is presented in Fig. 5b. The sorption of PET microplastics significantly increased as the pH value decreased within the range of 4, 6, 8, and 10: the sorption of virgin PET was 8.0, 5.3, 4.2 and 3.4 μg g^{-1}, and the sorption of aged PET was 22.4, 10.9, 6.5 and 4.9 μg g^{-1}, respectively. When the pH value decreased, the

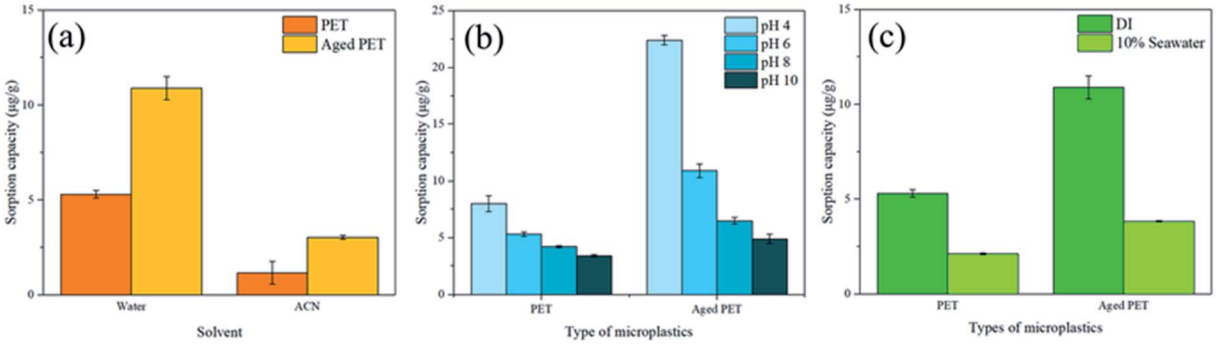

Fig. 5 Sorption capacity of virgin and aged PET microplastics for 4-MBC (a) in water and ACN, (b) at different pH values, and (c) in the presence of salinity ([4-MBC]$_0$ = 50 ppb, [microplastics]$_0$ = 100 mg, temperature = 20 °C, initial pH = 7 (with the exception of the control pH), salinity = 0 (with the exception of the salinity effect)).

carboxylic group (RCOOH) on the surface of the PET microplastics became more protonated, enhancing hydrogen bond formation and 4-MBC sorption.

Although a few studies[34,75,84] have mentioned that electrostatic attraction might play a key role in the sorption behavior of microplastics at different pH values, 4-MBC is nonionic in water due to its low solubility. Electrostatic attraction may not be the major mechanism behind the sorption behavior of 4-MBC on PET microplastics at different pH values. Further studies are needed to examine whether the sorption of any other non-ionizable contaminants onto microplastics is influenced by solution pH.

3.4.2 Effect of salinity. The sorption behavior in the presence of salinity may be affected by electrostatic effects owing to the competition sorption behavior between the metal ions and the sorbates, thereby reducing the sorption behavior of microplastics. The point of zero charge (pH_{PZC}) of the PET microplastic surface is approximately pH 4 (Table S9†); thus, metal ions are adsorbed onto PET microplastics, decreasing the active sorption sites (Fig. 5c). The sorption of virgin and aged PET microplastics was lower in the presence of salinity than in ultrapure water. The sorption of PET and aged PET was 2.11 and 3.83 μg g^{-1} in simulated seawater (0.35‰) and 5.3 and 10.9 μg g^{-1} in ultrapure water, respectively. These results further support the idea that hydrogen bond formation between 4-MBC and PET microplastics decreases under saline conditions and that 4-MBC sorption decreases at the same time due to the active sorption sites being occupied by metal ions in the monolayer sorption system.

3.5 Comparison of aging processes in natural sunlight and the laboratory

The environmental aging process may vary under different natural conditions due to the light source and climatic conditions. To verify the validity of the lab-aging experiment, an *in situ* aging process was applied to confirm whether the aging of plastic products will occur in the environment. Bot-PET samples were subjected to a natural sunlight aging process with predetermined sampling intervals (0, 3, 6, 9, and 12 months), and Env-PET samples were analyzed for comparison.

Fig. S6† shows the FTIR spectra of Bot-PET in the *in situ* aging process over 12 months. These results were similar to those of the laboratory experiments. The spectra indicate that the degree of aging of Bot-PET varied substantially between summer months (0 to 6 months) and winter months (6 to 12 months), where a peak at 3400 cm^{-1} associated with –OH group stretching, a peak at 1250 cm^{-1} associated with C–O stretching, a peaks at 2900 cm^{-1} associated with C–H bending and a peak at 1730 cm^{-1} associated with C═O stretching, respectively, were observed and increased in summer months.

In the Bot-PET experiment, the degree of aging of Bot-PET was found to be correlated with the sorption of 4-MBC. As the degree of aging is enhanced in summer months, sorption also increases. In contrast, when the degree of aging is stagnant in winter months, the sorption tends to be constant. This similarity could be attributed to the strong influence of weather on the aging of microplastics in the environment. Since the sorption of Env-PET was larger than that of Bot-PET (Table S10†), it could be inferred that 4-MBC sorption on PET bottles in the environment is underestimated.

3.6 Enhanced sorption behavior of aged PE and PP microplastics

Two other microplastics, PP and PE, were studied under the same experimental conditions to further investigate and support the enhanced sorption behavior of aged microplastics for 4-MBC. The results in Fig. S7† show that both PP and PE exhibited enhanced sorption of 4-MBC after the aging process, with the sorption of PP increasing from 19 to 28 μg g^{-1} and the sorption of PE increasing from 30 to 34 μg g^{-1}. The presence of oxygen-containing functional groups and the increased surface area could further enhance the sorption of both aged PP and PE microplastics compared with that of their virgin counterparts, similar to PET.

The effect of environmental factors on the sorption behavior of PP and PE microplastics was also studied. With regard to pH (Fig. S8a†), both PP and PE microplastics exhibited increased sorption under acidic conditions (the sorption of PP was 19.5 and 14.6 μg g^{-1} at pH 4 and 10, the sorption of aged PP was 30.8 and 19.6 μg g^{-1} at pH 4 and 10, the sorption of PE was 30.0 and

22.0 μg g^{-1} at pH 4 and 10, and the sorption of aged PE was 34.7 and 22.9 μg g^{-1} at pH 4 and 10, respectively). Regarding salinity, the metal ions in the simulated seawater also decreased the sorption of PP and PE microplastics, as shown in Fig. S8b† (in simulated seawater, the sorption of PP and aged PP was 18.3 and 22.0 μg g^{-1}, and the sorption of PE and aged PE was 27.3 and 28.4 μg g^{-1}, respectively; in ultrapure water, however, the sorption of PP and aged PP was 18.9 and 27.6 μg g^{-1}, and the sorption of PE and aged PE was 29.8 and 34.4 μg g^{-1}, respectively). Overall, in this work, the sorption enhancement of aged microplastics could be affected by hydrogen bond formation. Moreover, the increased sorption has a high correlation with salinity and pH on the sorption behavior of PET, PP and PE microplastics.

4. Conclusions

The increasingly widespread use of cosmetic plastic products raises the probability of environmental pollution in the form of UV filters such as 4-MBC. The results of the laboratory experiment show that the sorption equilibrium of 4-MBC onto PET microplastics is achieved within a day and that the sorption of aged PET microplastics (11 μg g^{-1}) is higher than that of virgin PET microplastics (5 μg g^{-1}). The sorption isotherm and kinetics of PET microplastics to 4-MBC are found to be Langmuir isotherm and pseudo-second order, in which aged PET has a higher sorption rate ($1.3 \times 10^5 > 1.1 \times 10^5$ g μg^{-1} h^{-1}). Moreover, hydrogen bonds between 4-MBC and RCOOH moieties are found to be the key factor affecting 4-MBC sorption onto aged PET microplastics. A much larger binding energy (48 kJ mol^{-1} *vs.* 28 kJ mol^{-1}) was observed between 4-MBC and the RCOOH moiety than between 4-MBC and the other oxygen-containing moieties (water, RCHO and RCOH) according to the DFT calculation results.

Hydrogen bonds are affected by different environmental conditions, such as pH, salinity, and solar irradiance. When the pH value decreases from 10 to 4, the sorption of PET microplastics increases due to the increase in the number of protonated carboxylic groups on their surface under acidic conditions (the sorption of PET ranges from 8.0 to 3.4 μg g^{-1}, and the sorption of aged PET ranges from 22 to 5 μg g^{-1}). On the other hand, under simulated seawater conditions, the sorption of PET microplastics decreases in the presence of salinity (the sorption of PET ranges from 5.3 to 2.1 μg g^{-1}, and the sorption of aged PET ranges from 11 to 4 μg g^{-1}). In the natural sunlight aging experiment, the microplastics obviously deteriorated under the long duration of sunlight exposure, thereby increasing sorption (the sorption of Bot-PET ranges from 0.4 to 0.8 μg g^{-1} after 6 months of sunlight exposure).

In this work, two possible ways to determine the formation of hydrogen bonds during sorption were also revealed. In experiments, observing the sorption behavior in an acetonitrile solution could be a potential way to evaluate hydrogen bonds. In theory, DFT is regarded as a reliable tool for detecting hydrogen bond formation. Due to the higher sorption capacity of aged microplastics than virgin microplastics, aged microplastics exhibit enhanced sorption behavior and can therefore cause more adverse effects on the environment than virgin microplastics, as their presence not only results in higher contaminant persistence but also increases the mobility of contaminants in the environment. Furthermore, the enhanced mobility of microplastics that uptake contaminants will increase the transport of contaminants into the soil and organisms. To evaluate the risk of aged microplastics to the environment, the sorption mechanism of contaminants onto aged microplastics and the potential hazards of aged microplastics with fully adsorbed contaminants in the environment should be further investigated.

Author contributions

Chun-Yu Shih: writing—original draft, conceptualization, methodology, visualization, investigation.

Yu-Hsiang Wang: methodology, visualization, writing—review and editing.

Yi-Ju Chen: conceptualization, visualization.

Hsin-An Chen: density functional theory – visualization, writing—review and editing.

Angela Yu-Chen Lin: supervision, validation, writing—review and editing, funding acquisition.

Conflicts of interest

There are no conflicts to declare.

Acknowledgements

This work was financially supported by the Ministry of Science and Technology through the project MOST (108-2221-E-002-122-MY3, 108-2221-E-002-123-MY3) in Taiwan.

References

1 S. Lambert and M. Wagner, Microplastics are contaminants of emerging concern in freshwater environments: an overview, in *Freshwater microplastics*, Springer, Cham, 2018, pp. 1–23.

2 L. G. A. Barboza, A. D. Vethaak, B. R. Lavorante, A.-K. Lundebye and L. Guilhermino, Marine microplastic debris: An emerging issue for food security, food safety and human health, *Mar. Pollut. Bull.*, 2018, **133**, 336–348.

3 M. Lehtiniemi, S. Hartikainen, P. Näkki, J. Engström-Öst, A. Koistinen and O. Setälä, Size matters more than shape: Ingestion of primary and secondary microplastics by small predators, *Food Webs*, 2018, **17**, e00097.

4 T. S. M. Amelia, W. M. A. W. M. Khalik, M. C. Ong, Y. T. Shao, H.-J. Pan and K. Bhubalan, Marine microplastics as vectors of major ocean pollutants and its hazards to the marine ecosystem and humans, *Progress in Earth and Planetary Science*, 2021, **8**(1), 1–26.

5 D. Boyle, A. I. Catarino, N. J. Clark and T. B. Henry, Polyvinyl chloride (PVC) plastic fragments release Pb additives that are bioavailable in zebrafish, *Environ. Pollut.*, 2020, **263**, 114422.

6 M. A. Browne, S. J. Niven, T. S. Galloway, S. J. Rowland and R. C. Thompson, Microplastic moves pollutants and additives to worms, reducing functions linked to health and biodiversity, *Curr. Biol.*, 2013, **23**(23), 2388–2392.

7 S. Zhang, B. Han, Y. Sun and F. Wang, Microplastics influence the adsorption and desorption characteristics of Cd in an agricultural soil, *J. Hazard. Mater.*, 2020, **388**, 121775.

8 T. Hüffer, A.-K. Weniger and T. Hofmann, Sorption of organic compounds by aged polystyrene microplastic particles, *Environ. Pollut.*, 2018, **236**, 218–225.

9 S. Klein, I. K. Dimzon, J. Eubeler and T. P. Knepper, Analysis, occurrence, and degradation of microplastics in the aqueous environment, in *Freshwater microplastics*, Springer, Cham, 2018, pp. 51–67.

10 X. Fan, Y. Zou, N. Geng, J. Liu, J. Hou, D. Li, C. Yang and Y. Li, Investigation on the adsorption and desorption behaviors of antibiotics by degradable MPs with or without UV ageing process, *J. Hazard. Mater.*, 2020, 123363.

11 F. Gao, J. Li, C. Sun, L. Zhang, F. Jiang, W. Cao and L. Zheng, Study on the capability and characteristics of heavy metals enriched on microplastics in marine environment, *Mar. Pollut. Bull.*, 2019, **144**, 61–67.

12 M. Lang, X. Yu, J. Liu, T. Xia, T. Wang, H. Jia and X. Guo, Fenton aging significantly affects the heavy metal adsorption capacity of polystyrene microplastics, *Sci. Total Environ.*, 2020, 137762.

13 S. Tang, L. Lin, X. Wang, A. Feng and A. Yu, Pb (II) uptake onto nylon microplastics: Interaction mechanism and adsorption performance, *J. Hazard. Mater.*, 2020, **386**, 121960.

14 J. Brandon, M. Goldstein and M. D. Ohman, Long-term aging and degradation of microplastic particles: Comparing *in situ* oceanic and experimental weathering patterns, *Mar. Pollut. Bull.*, 2016, **110**(1), 299–308.

15 L. Ding, R. Mao, S. Ma, X. Guo and L. Zhu, High temperature depended on the ageing mechanism of microplastics under different environmental conditions and its effect on the distribution of organic pollutants, *Water Res.*, 2020, **174**, 115634.

16 J. Liu, T. Zhang, L. Tian, X. Liu, Z. Qi, Y. Ma, R. Ji and W. Chen, Aging significantly affects mobility and contaminant-mobilizing ability of nanoplastics in saturated loamy sand, *Environ. Sci. Technol.*, 2019, **53**(10), 5805–5815.

17 P. Liu, L. Qian, H. Wang, X. Zhan, K. Lu, C. Gu and S. Gao, New insights into the aging behavior of microplastics accelerated by advanced oxidation processes, *Environ. Sci. Technol.*, 2019, **53**(7), 3579–3588.

18 D. Brennecke, B. Duarte, F. Paiva, I. Caçador and J. Canning-Clode, Microplastics as vector for heavy metal contamination from the marine environment, *Estuarine, Coastal Shelf Sci.*, 2016, **178**, 189–195.

19 Q. Chen, H. Zhang, A. Allgeier, Q. Zhou, J. D. Ouellet, S. E. Crawford, Y. Luo, Y. Yang, H. Shi and H. Hollert, Marine microplastics bound dioxin-like chemicals: Model explanation and risk assessment, *J. Hazard. Mater.*, 2019, **364**, 82–90.

20 R. J. Vroom, A. A. Koelmans, E. Besseling and C. Halsband, Aging of microplastics promotes their ingestion by marine zooplankton, *Environ. Pollut.*, 2017, **231**, 987–996.

21 K. Fent, P. Y. Kunz, A. Zenker and M. Rapp, A tentative environmental risk assessment of the UV-filters 3-(4-methylbenzylidene-camphor), 2-ethyl-hexyl-4-trimethoxycinnamate, benzophenone-3, benzophenone-4 and 3-benzylidene camphor, *Mar. Environ. Res.*, 2010, **69**, S4–S6.

22 W.-K. Ho, J. C.-F. Law, T. Zhang and K. S.-Y. Leung, Effects of Weathering on the Sorption Behavior and Toxicity of Polystyrene Microplastics in Multi-solute Systems, *Water Res.*, 2020, **187**, 116419.

23 W.-K. Ho and K. S.-Y. Leung, Sorption and desorption of organic UV filters onto microplastics in single and multi-solute systems, *Environ. Pollut.*, 2019, **254**, 113066.

24 F. G. Torres, D. C. Dioses-Salinas, C. I. Pizarro-Ortega and G. E. De-la-Torre, Sorption of chemical contaminants on degradable and non-degradable microplastics: Recent progress and research trends, *Sci. Total Environ.*, 2020, 143875.

25 C. Wu, K. Zhang, X. Huang and J. Liu, Sorption of pharmaceuticals and personal care products to polyethylene debris, *Environ. Sci. Pollut. Res.*, 2016, **23**(9), 8819–8826.

26 L. Chen, X. Li, H. Hong and D. Shi, Multigenerational effects of 4-methylbenzylidene camphor (4-MBC) on the survival, development and reproduction of the marine copepod Tigriopus japonicus, *Aquat. Toxicol.*, 2018, **194**, 94–102.

27 M. Liang, S. Yan, R. Chen, X. Hong and J. Zha, 3-(4-Methylbenzylidene) camphor induced reproduction toxicity and antiandrogenicity in Japanese medaka (Oryzias latipes), *Chemosphere*, 2020, **249**, 126224.

28 I. Ozáez, J. L. Martínez-Guitarte and G. Morcillo, Effects of *in vivo* exposure to UV filters (4-MBC, OMC, BP-3, 4-HB, OC, OD-PABA) on endocrine signaling genes in the insect Chironomus riparius, *Sci. Total Environ.*, 2013, **456**, 120–126.

29 S.-C. Hsieh, W. W.-P. Lai and A. Y.-C. Lin, Kinetics and mechanism of 4-methylbenzylidene camphor degradation by UV-activated persulfate oxidation, *Environ. Sci. Pollut. Res.*, 2021, **28**(14), 18021–18034.

30 W. W.-P. Lai, K.-L. Chen and A. Y.-C. Lin, Solar photodegradation of the UV filter 4-methylbenzylidene camphor in the presence of free chlorine, *Sci. Total Environ.*, 2020, 137860.

31 R. Rodil, M. Moeder, R. Altenburger and M. Schmitt-Jansen, Photostability and phytotoxicity of selected sunscreen agents and their degradation mixtures in water, *Anal. Bioanal. Chem.*, 2009, **395**(5), 1513.

32 R. Beiras, S. Muniategui-Lorenzo, R. Rodil, T. Tato, R. Montes, S. López-Ibáñez, E. Concha-Graña, P. Campoy-López, N. Salgueiro-González and J. B. Quintana, Polyethylene microplastics do not increase bioaccumulation or toxicity of nonylphenol and 4-MBC to marine zooplankton, *Sci. Total Environ.*, 2019, **692**, 1–9.

33 T. Hüffer and T. Hofmann, Sorption of non-polar organic compounds by micro-sized plastic particles in aqueous solution, *Environ. Pollut.*, 2016, **214**, 194–201.
34 G. Liu, Z. Zhu, Y. Yang, Y. Sun, F. Yu and J. Ma, Sorption behavior and mechanism of hydrophilic organic chemicals to virgin and aged microplastics in freshwater and seawater, *Environ. Pollut.*, 2019, **246**, 26–33.
35 P. Liu, K. Lu, J. Li, X. Wu, L. Qian, M. Wang and S. Gao, Effect of aging on adsorption behavior of polystyrene microplastics for pharmaceuticals: Adsorption mechanism and role of aging intermediates, *J. Hazard. Mater.*, 2020, **384**, 121193.
36 X. Liu, P. Sun, G. Qu, J. Jing, T. Zhang, H. Shi and Y. Zhao, Insight into the characteristics and sorption behaviors of aged polystyrene microplastics through three type of accelerated oxidation processes, *J. Hazard. Mater.*, 2021, **407**, 124836.
37 A. Müller, R. Becker, U. Dorgerloh, F.-G. Simon and U. Braun, The effect of polymer aging on the uptake of fuel aromatics and ethers by microplastics, *Environ. Pollut.*, 2018, **240**, 639–646.
38 J. Wu, P. Xu, Q. Chen, D. Ma, W. Ge, T. Jiang and C. Chai, Effects of polymer aging on sorption of 2, 2′, 4, 4′-tetrabromodiphenyl ether by polystyrene microplastics, *Chemosphere*, 2020, 126706.
39 X. Guo and J. Wang, Sorption of antibiotics onto aged microplastics in freshwater and seawater, *Mar. Pollut. Bull.*, 2019, **149**, 110511.
40 H. Zhang, J. Wang, B. Zhou, Y. Zhou, Z. Dai, Q. Zhou, P. Chriestie and Y. Luo, Enhanced adsorption of oxytetracycline to weathered microplastic polystyrene: Kinetics, isotherms and influencing factors, *Environ. Pollut.*, 2018, **243**, 1550–1557.
41 L. Zhou, T. Wang, G. Qu, H. Jia and L. Zhu, Probing the aging processes and mechanisms of microplastic under simulated multiple actions generated by discharge plasma, *J. Hazard. Mater.*, 2020, **398**, 122956.
42 X. Wu, P. Liu, H. Huang and S. Gao, Adsorption of triclosan onto different aged polypropylene microplastics: Critical effect of cations, *Sci. Total Environ.*, 2020, **717**, 137033.
43 L. A. Holmes, A. Turner and R. C. Thompson, Adsorption of trace metals to plastic resin pellets in the marine environment, *Environ. Pollut.*, 2012, **160**, 42–48.
44 Y. Wang, X. Wang, Y. Li, J. Li, Y. Liu, S. Xia and J. Zhao, Effects of exposure of polyethylene microplastics to air, water and soil on their adsorption behaviors for copper and tetracycline, *Chem. Eng. J.*, 2021, **404**, 126412.
45 Z.-Z. Bao, Z.-F. Chen, Y. Zhong, G. Wang, Z. Qi and Z. Cai, Adsorption of phenanthrene and its monohydroxy derivatives on polyvinyl chloride microplastics in aqueous solution: Model fitting and mechanism analysis, *Sci. Total Environ.*, 2021, **764**, 142889.
46 Y. Wang, X. Wang, Y. Li, J. Li, F. Wang, S. Xia and J. Zhao, Biofilm alters tetracycline and copper adsorption behaviors onto polyethylene microplastics, *Chem. Eng. J.*, 2020, **392**, 123808.
47 J. Ireta, J. Neugebauer and M. Scheffler, On the accuracy of DFT for describing hydrogen bonds: dependence on the bond directionality, *J. Phys. Chem. A*, 2004, **108**(26), 5692–5698.
48 B. Oliveira, F. Pereira, R. de Araújo and M. Ramos, The hydrogen bond strength: New proposals to evaluate the intermolecular interaction using DFT calculations and the AIM theory, *Chem. Phys. Lett.*, 2006, **427**(1–3), 181–184.
49 M. V. Vener, A. Egorova, A. V. Churakov and V. G. Tsirelson, Intermolecular hydrogen bond energies in crystals evaluated using electron density properties: DFT computations with periodic boundary conditions, *J. Comput. Chem.*, 2012, **33**(29), 2303–2309.
50 R. Pinal, P. S. C. Rao, L. S. Lee, P. V. Cline and S. H. Yalkowsky, Cosolvency of partially miscible organic solvents on the solubility of hydrophobic organic chemicals, *Environ. Sci. Technol.*, 1990, **24**(5), 639–647.
51 G. Kresse and J. Hafner, Ab initio molecular dynamics for liquid metals, *Phys. Rev. B: Condens. Matter Mater. Phys.*, 1993, **47**(1), 558.
52 G. Kresse and J. Hafner, Ab initio molecular dynamics for open-shell transition metals, *Phys. Rev. B: Condens. Matter Mater. Phys.*, 1993, **48**(17), 13115.
53 G. Kresse and J. Hafner, Ab initio molecular-dynamics simulation of the liquid-metal–amorphous-semiconductor transition in germanium, *Phys. Rev. B: Condens. Matter Mater. Phys.*, 1994, **49**(20), 14251.
54 J. P. Perdew, J. A. Chevary, S. H. Vosko, K. A. Jackson, M. R. Pederson, D. J. Singh and C. Fiolhais, Atoms, molecules, solids, and surfaces: Applications of the generalized gradient approximation for exchange and correlation, *Phys. Rev. B: Condens. Matter Mater. Phys.*, 1992, **46**(11), 6671.
55 J. P. Perdew and Y. Wang, Accurate and simple analytic representation of the electron-gas correlation energy, *Phys. Rev. B: Condens. Matter Mater. Phys.*, 1992, **45**(23), 13244.
56 P. E. Blöchl, Projector augmented-wave method, *Phys. Rev. B: Condens. Matter Mater. Phys.*, 1994, **50**(24), 17953.
57 G. Kresse and D. Joubert, From ultrasoft pseudopotentials to the projector augmented-wave method, *Phys. Rev. B: Condens. Matter Mater. Phys.*, 1999, **59**(3), 1758.
58 S. Grimme, J. Antony, S. Ehrlich and H. Krieg, A consistent and accurate *ab initio* parametrization of density functional dispersion correction (DFT-D) for the 94 elements H-Pu, *J. Chem. Phys.*, 2010, **132**(15), 154104.
59 S. Grimme, S. Ehrlich and L. Goerigk, Effect of the damping function in dispersion corrected density functional theory, *J. Comput. Chem.*, 2011, **32**(7), 1456–1465.
60 Q. Wang, Y. Zhang, X. Wangjin, Y. Wang, G. Meng and Y. Chen, The adsorption behavior of metals in aqueous solution by microplastics effected by UV radiation, *J. Environ. Sci.*, 2020, **87**, 272–280.
61 B. Gewert, M. M. Plassmann and M. MacLeod, Pathways for degradation of plastic polymers floating in the marine environment, *Environ. Sci.: Processes Impacts*, 2015, **17**(9), 1513–1521.
62 J. White and A. Turnbull, Weathering of polymers: mechanisms of degradation and stabilization, testing strategies and modelling, *J. Mater. Sci.*, 1994, **29**(3), 584–613.

63 G. Wypych, *Handbook of material weathering*, Elsevier, 2018.
64 T. A. Saleh, The influence of treatment temperature on the acidity of MWCNT oxidized by HNO3 or a mixture of HNO3/H2SO4, *Appl. Surf. Sci.*, 2011, **257**(17), 7746–7751.
65 T. A. Saleh, Simultaneous adsorptive desulfurization of diesel fuel over bimetallic nanoparticles loaded on activated carbon, *J. Cleaner Prod.*, 2018, **172**, 2123–2132.
66 H. Luo, Y. Li, Y. Zhao, Y. Xiang, D. He and X. Pan, Effects of accelerated aging on characteristics, leaching, and toxicity of commercial lead chromate pigmented microplastics, *Environ. Pollut.*, 2020, **257**, 113475.
67 T. A. Saleh, M. Tuzen and A. Sarı, Polyethylenimine modified activated carbon as novel magnetic adsorbent for the removal of uranium from aqueous solution, *Chem. Eng. Res. Des.*, 2017, **117**, 218–227.
68 M. Tuzen, T. A. Saleh and A. Sarı, Interfacial polymerization of trimesoyl chloride with melamine and palygorskite for efficient uranium ions ultra-removal, *Chem. Eng. Res. Des.*, 2020, **159**, 353–361.
69 F. Zare, M. Ghaedi, A. Daneshfar, S. Agarwal, I. Tyagi, T. A. Saleh and V. K. Gupta, Efficient removal of radioactive uranium from solvent phase using AgOH–MWCNTs nanoparticles: Kinetic and thermodynamic study, *Chem. Eng. J.*, 2015, **273**, 296–306.
70 Z. Li, X. Hu, L. Qin and D. Yin, Evaluating the effect of different modified microplastics on the availability of polycyclic aromatic hydrocarbons, *Water Res.*, 2020, **170**, 115290.
71 J. Li, K. Zhang and H. Zhang, Adsorption of antibiotics on microplastics, *Environ. Pollut.*, 2018, **237**, 460–467.
72 M. M. Rashad, I. E. El-Sayed, A. A. Galhoum, M. M. Abdeen, H. I. Mira, E. A. Elshehy, S. Zhang, X. Lu, J. Xin and E. Guibal, Synthesis of α-aminophosphonate based sorbents–Influence of inserted groups (carboxylic *vs.* amine) on uranyl sorption, *Chem. Eng. J.*, 2021, **421**, 127830.
73 S. Saoiabi, K. Achelhi, S. Masse, A. Saoiabi, A. Laghzizil and T. Coradin, Organo-apatites for lead removal from aqueous solutions: a comparison between carboxylic acid and aminophosphonate surface modification, *Colloids Surf., A*, 2013, **419**, 180–185.
74 H. Koyuncu, A. R. Kul, N. Yıldız, A. Çalımlı and H. Ceylan, Equilibrium and kinetic studies for the sorption of 3-methoxybenzaldehyde on activated kaolinites, *J. Hazard. Mater.*, 2007, **141**(1), 128–139.
75 B. Xu, F. Liu, P. C. Brookes and J. Xu, The sorption kinetics and isotherms of sulfamethoxazole with polyethylene microplastics, *Mar. Pollut. Bull.*, 2018, **131**, 191–196.
76 A. Bakir, S. J. Rowland and R. C. Thompson, Competitive sorption of persistent organic pollutants onto microplastics in the marine environment, *Mar. Pollut. Bull.*, 2012, **64**(12), 2782–2789.
77 B. Xu, F. Liu, P. C. Brookes and J. Xu, Microplastics play a minor role in tetracycline sorption in the presence of dissolved organic matter, *Environ. Pollut.*, 2018, **240**, 87–94.
78 I. Langmuir, The adsorption of gases on plane surfaces of glass, mica and platinum, *J. Am. Chem. Soc.*, 1918, **40**(9), 1361–1403.
79 H. Swenson and N. P. Stadie, Langmuir's theory of adsorption: A centennial review, *Langmuir*, 2019, **35**(16), 5409–5426.
80 S. Wang, L. Kong, J. Long, M. Su, Z. Diao, X. Chang, D. Chen, G. Song and K. Shih, Adsorption of phosphorus by calcium-flour biochar: Isotherm, kinetic and transformation studies, *Chemosphere*, 2018, **195**, 666–672.
81 H. Cao, X. Wu, S. S. A. Syed-Hassan, S. Zhang, S. H. Mood, Y. J. Milan and M. Garcia-Perez, Characteristics and mechanisms of phosphorous adsorption by rape straw-derived biochar functionalized with calcium from eggshell, *Bioresour. Technol.*, 2020, **318**, 124063.
82 I. Ahmed and S. H. Jhung, Applications of metal-organic frameworks in adsorption/separation processes *via* hydrogen bonding interactions, *Chem. Eng. J.*, 2017, **310**, 197–215.
83 N. N. Casillas-Ituarte and H. C. Allen, Water, chloroform, acetonitrile, and atrazine adsorption to the amorphous silica surface studied by vibrational sum frequency generation spectroscopy, *Chem. Phys. Lett.*, 2009, **483**(1–3), 84–89.
84 X. Guo, J. Pang, S. Chen and H. Jia, Sorption properties of tylosin on four different microplastics, *Chemosphere*, 2018, **209**, 240–245.